Theor Chem Acc (2001) 106:146–151
DOI 10.1007/s002140000246

Theoretical
Chemistry Accounts

Regular article

Quantum mechanical/molecular mechanical study of three stationary points along the deacylation step of the catalytic mechanism of elastase

Maya Topf, Péter Várnai, W. Graham Richards

Physical and Theoretical Chemistry Laboratory, Oxford University, Oxford OX1 3QT, UK

Received: 11 September 2000 / Accepted: 15 September 2000 / Published online: 21 March 2001

Abstract. A large amount of experimental as well as theoretical information is available about the mechanism of serine proteases, but many questions remain unanswered. Here we study the deacylation step of the reaction mechanism of elastase. The water molecule in the acyl-enzyme active site, the binding mode of the carbonyl oxygen in the oxyanion hole, the characteristics of the tetrahedral intermediate structure, and the mobility of the imidazole ring of His-57 were studied with quantum mechanical/molecular mechanical methods. The models are based on a recent high-resolution crystal structure of the acyl-enzyme intermediate. The nucleophilic water in the active site of the acyl-enzyme has been shown to have two minima that differ by only 2 kcalmol^{-1} in energy. The carbonyl group of the acyl-enzyme is located in the oxyanion hole and is positioned for attack by the hydrolytic water. The tetrahedral intermediate is a weakly bonded system, which is electrostatically stabilized by short hydrogen bonds to the backbone NH groups of Gly-193 and Ser-195 in the oxyanion hole. The short distance between the $N^{\varepsilon 2}$ of His-57 and the O^{γ} of Ser-195 in the tetrahedral intermediate indicates a small movement of the imidazole ring towards the product in the deacylation step. The carbonyl group of the enzyme-product complex is not held strongly in the oxyanion hole, which shows that the peptide is first released from the oxyanion hole before it leaves the active site to regenerate the native state of the enzyme.

Key words: Quantum mechanical/molecular mechanical calculations – Serine protease – Elastase – Theoretical reaction mechanism – Tetrahedral intermediate

Correspondence to: W. G. Richards;
e-mail: graham.richards@chem.ox.ac.uk

Contribution to the Symposium Proceedings of Computational Biophysics 2000

1 Introduction

Serine proteases are important enzymes in many biological systems owing to their ability to hydrolyze substrates which contain ester or amide groups. The catalytic mechanism of these enzymes has been investigated extensively by experimental [1] and theoretical methods [2]. One family of such enzymes is the chymotrypsin family, whose members have a fold that consists of two antiparallel β-barrel domains. A conserved catalytic triad of serine, histidine, and aspartate residues is situated in a crevice between the domains [3, 4]. These residues are Ser-195, His-57, and Asp-102, using the numbering of chymotrypsinogen.

The catalytic mechanism of serine proteases has two main steps: acylation to form a covalently bonded acyl-enzyme(EA) intermediate and deacylation to reproduce the free enzyme [3, 4]. Most theoretical studies have dealt only with the acylation step and not with the deacylation step, which is rate-determining for certain ester substrates [5].

Deacylation is initiated by the attack of a water molecule on the EA carbonyl group. This nucleophilic attack has been suggested to lead to a tetrahedral intermediate (TI2), which then collapses to yield the enzyme-product complex (EP) [1]. The "oxyanion hole", which consists of the two backbone NH groups of Ser-195 and Gly-193, stabilizes the negative charge developed on the carbonyl oxygen in the TI2 [6, 7, 8, 9]. During the nucleophilic attack, the imidazole base of His-57 acts as a general base: it abstracts a proton from the hydrolytic water, which increases its nucleophilicity and leads to an attack of the carbonyl carbon. Subsequently, the protonated imidazolium acts as a general acid by donating a proton to O^{γ} of Ser-195, which leads to the collapse of the TI2. The mobility of the histidine ring is important for providing an ideal orientation for the proton transfer [10, 11, 12]. Asp-102 has been proposed to provide electrostatic stabilization of the protonated form of His-57 [9, 13], but the nature of the hydrogen bond between them continues to be the subject of controversy [14, 15, 16, 17].

Some questions about the EA intermediate remain unanswered. For example, the mode of binding of the carbonyl oxygen of the EA in the oxyanion hole is not clear. Some studies indicate that the carbonyl oxygen is hydrogen bonded to the backbone NH groups of Ser-195 and Gly-193 [18, 19, 20, 21], while others reveal no such interaction [6]. The way in which the hydrolytic water binds in the EA active site is also not clear [6, 22, 23].

An additional important question concerning the nature of the mechanism of serine proteases is whether the deacylation step is concerted or stepwise [8, 24]. A concerted mechanism involves a tetrahedral transition state in which one of the protons of the hydrolytic water is not fully transferred to $N^{\varepsilon 2}$ of His-57 before it is abstracted by O^{γ} of Ser-195 to break the EA structure. In a stepwise mechanism, a proton is first fully transferred from the hydrolytic water to $N^{\varepsilon 2}$, and a TI2 is formed. This step is followed by a proton transfer from His-57 to Ser-195 to regenerate the native state of the enzyme as the carboxylic acid product is formed by breaking the bond between O^{γ} of Ser-195 and the carbonyl carbon. Even though there is only indirect evidence for the existence of a tedrahedral intermediate in both acylation and deacylation steps [25, 26, 27], modeling it has proved useful [13, 22, 28]. Typically, the energy of this intermediate is assumed to be close to the energy of the transition state, on the basis of the Hammond postulate.

In the present work we assume a stepwise mechanism and give details on three stationary points along the reaction pathway of the deacylation step: the EA, the TI2, and the EP complex. The recent high-resolution crystal structure of the EA intermediate of porcine pancreatic elastase (PPE) with the natural heptapeptide human β-casomorphin-7 (BCM7) [21] is used. The structure contains the four last residues of the β-strand substrate: Val-Glu-Pro-Ile. The isoleucine is connected to Ser-195 of the enzyme via an ester bond. The ester carbonyl is located in the oxyanion hole with hydrogen-bond distances from the oxygen to the backbone NH groups of Gly-193 and Ser-195 of 2.9 Å in both cases. A well-defined water molecule is equidistant between the carbon of the ester carbonyl and $N^{\varepsilon 2}$ of His-57.

A combined QM/MM method [29, 30] was employed to describe the enzyme active site. Charge distributions, bond orders, and geometric parameters were obtained for the three stationary points. These provide a better understanding of the location of the hydrolytic water molecule in the EA structure, the binding mode of the carbonyl oxygen in the oxyanion hole, the characteristics of the TI2 structure, and the mobility of the imidazole ring of His-57.

2 Methods

The EA crystal structure of the natural heptapeptide substrate, BCM7, and PPE [21] was retrieved as entry 1QIX of the Brookhaven Protein Data Bank [31].

Hydrogens were added to the complex using the HBUILD routine of CHARMM (version 27) [32]. The standard all-atom parameters [33] were used for the whole system except for the acylated Ser-195. The parameters for this fragment were derived using a mixture of CHARMM atom types; the charges were calculated by fitting to the HF/6-31G* electrostatic potential of methyl acetate in vacuum [34], using the program Gaussian98 [35]. For nonbonded interactions, the van der Waals terms were truncated with a switch function between 10 and 14 Å and the electrostatic terms with a shift function with a cutoff distance of 14 Å [32]; the dielectric constant was unity.

All crystallographic water molecules were deleted except for the hydrolytic water molecule in the active site of the protein. Water molecules were added to the complex by superimposing a 30-Å sphere of TIP3P water molecules [36] centered at the reactive carbonyl carbon of the peptide (C_{acyl}). Any water molecule whose oxygen was within 2.8 Å of any heavy atom of the EA was removed. The water molecules and the protein hydrogens were minimized and then equilibrated at 300 K for 5 ps, while keeping the remaining protein atoms fixed. The equilibration was performed using the stochastic boundary conditions [37] with a time step of 2 fs, a friction coefficient of 62 ps^{-1} for the water oxygens [38], and the SHAKE algorithm [39]. The original 30-Å sphere of TIP3P water molecules was rotated 90° and the previous solvation procedure was repeated. The final system contained 240 protein residues, the four-residue substrate, the hydrolytic crystal water, and 2800 added water molecules, with a total of 12,053 atoms.

For the stochastic boundary MD simulation of the complete system, the atoms were divided into a reaction region, which contained all residues within 18 Å of the carbonyl carbon, and a buffer region, which contained the rest of the system. The frictional coefficients for water oxygen and heavy atoms in the protein were 62 and 200 ps^{-1}, respectively [38]. The complete system was minimized to relax the crystal structure. Langevin dynamics was then performed for 50 ps and the final structure was minimized with 200 steps of the steepest descent (SD) method followed by 2000 steps of the adopted basis Newton–Raphson (ABNR) method [32]. The root-mean-square (rms) deviation of the atomic positions in the final structure from those in the crystal structure was 0.9 Å. This minimized structure was used as a starting point for the subsequent quantum mechanical/molecular mechanical (QM/MM) minimizations of three stationary points along the reaction pathway of the deacylation step: the EA, the TI2, and the EP complex (Fig. 1).

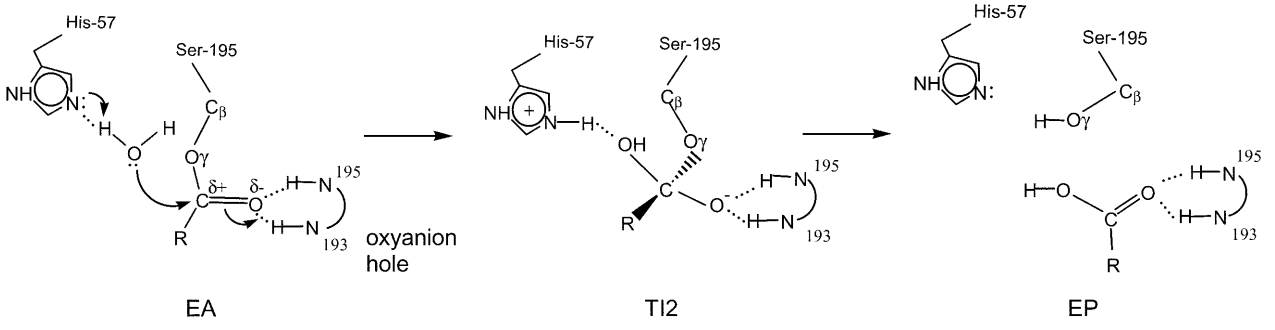

Fig. 1. Schematic representation of the reaction pathway of the deacylation step of serine protease catalysis: acyl-enzyme (*EA*), tetrahedral intermediate (*TI2*), enzyme-product (*EP*) complex

Two models of the EA structure were prepared (Fig. 2). The first model, EA-1, was obtained from the minimization that followed the MD simulation in which one hydrogen of the hydrolytic water molecule (H^1_{wat}) was hydrogen bonded to the catalytic nitrogen atom of His-57 ($N^{\varepsilon 2}$) and the other (H^2_{wat}) to bulk water. The second model, EA-2, was prepared such that the hydrolytic water molecule forms a hydrogen-bonded bridge between the carbonyl oxygen (O_{acyl}) and $N^{\varepsilon 2}$ of His-57. One of the hydrogens of the hydrolytic water (H^2_{wat}) was manually placed between the water oxygen and the carbonyl oxygen and was constrained there during a 7-ps MD simulation followed by minimization. The other hydrogen (H^1_{wat}) was not constrained but maintained its hydrogen bond to $N^{\varepsilon 2}$ during the simulation. The TI2 was prepared by manually moving $H^1{}_{wat}$ to $N^{\varepsilon 2}$ of His-57, and the remaining hydroxyl was added to the peptide carbonyl carbon (C_{acyl}). The EP complex was prepared by breaking the EA bond between O^{γ} of Ser-195 and C_{acyl} and adding the water hydrogen $H^1{}_{wat}$ to O^{γ}. The remaining hydroxyl group was added to the carbonyl carbon to form the peptide C terminus.

To have an improved description of the highly polarized catalytic region of elastase, a combined QM/MM potential was used to perform minimizations of the three structures along the reaction pathway. In the QM/MM method the central active site of the enzyme is described by a QM potential and the influence of the remainder of the protein is taken into account by a coupled MM potential. The QM region was treated with Hartree–Fock theory (HF) using the 3-21G and 6-31G* basis sets. The calculations were performed using the program GAMESS-US [40] implemented within CHARMM [41].

The QM region included the imidazole ring of His-57, a fragment of the peptide including the reactive carbonyl group, fragments of Gln-192, Gly-193, Asp-194, and Ser-195, and the hydrolytic water molecule (Fig. 3). Link atoms were added to each of the structures to satisfy the valence of the QM part and were treated as hydrogen atoms that did not interact with the MM region [30]. In total, 49 atoms, including six link atoms, were treated quantum mechanically and 12,010 atoms were treated molecular mechanically. The QM/MM minimizations included the SD method followed by the ABNR method until the average rms gradient was less than 0.1 $kcalmol^{-1}Å^{-1}$.

Energies and geometric parameters of the enzyme were obtained from the minimizations to understand the characteristics of the three stationary points along the reaction path of the deacylation step. The energies were calculated for the QM region of the enzyme including polarization due to the MM environment. Bond orders and charges from the QM/MM wavefunction were calculated by the natural bond orbital (NBO) analysis [42] implemented in Gaussian98 [35].

3 Results and discussion

We present a detailed analysis of the QM/MM minimizations of the three stationary points involved in the deacylation step: the EA, the TI2, and the EP complex. The models are based on the final structure obtained from a MD simulation on the EA crystal structure. During the whole simulation the hydrolytic water molecule remained in the active site, while bulk water molecules exchanged locations extensively. This is in contrast to a MD simulation of acyl-chymotrypsin, which showed that the hydrolytic water molecule exchanges with the bulk solvent [23].

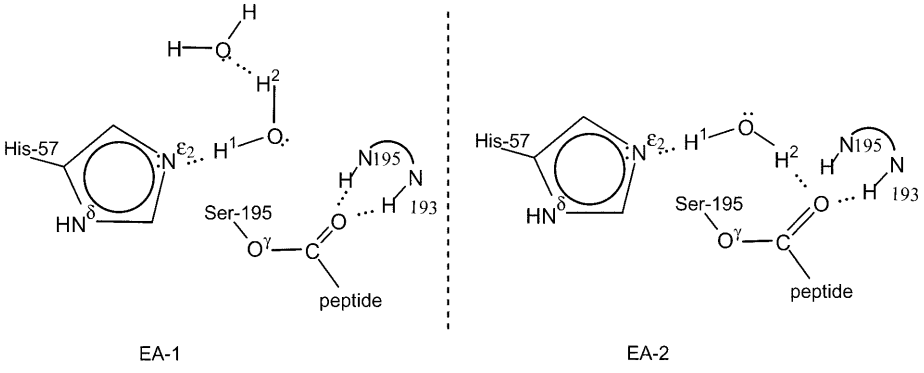

Fig. 2. Schematic representation of the two models of the EA. In the first model (*EA-1*) one hydrogen of the hydrolytic water molecule (H^1_{wat}) is hydrogen bonded to the catalytic nitrogen atom of His-57 ($N^{\varepsilon 2}$) and the other (H^2_{wat}) is bonded to bulk water. In the second model (*EA-2*) the hydrolytic water molecule forms a hydrogen-bond bridge between the carbonyl oxygen (O_{acyl}) and $N^{\varepsilon 2}$ of His-57

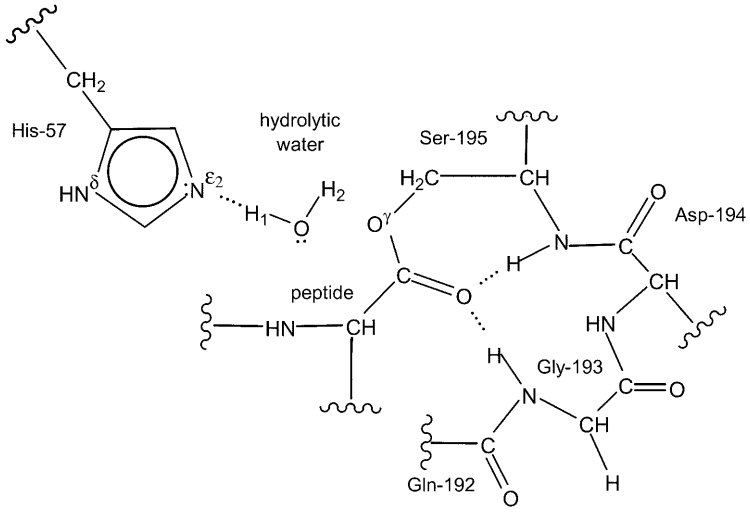

Fig. 3. The quantum mechanical region used in the minimizations of the three states of the deacylation step: the EA, the TI2, and the EP complex. This 49-atom region includes the imidazole ring of His-57, a fragment of the peptide including the reactive carbonyl group, fragments of Gln-192, Gly-193, Asp-194, and Ser-195, the hydrolytic water molecule, and an additional six link atoms

Selected charges of the atoms involved in the reaction (Table 1) and bond orders (Table 2) were obtained from an NBO analysis of the HF/3-21G and HF/6-31G* wavefunctions determined in the presence of the MM charges. Distances, bond angles, and dihedrals angles (Table 3) were calculated for each minimized structure at both HF levels. Although the results obtained from the (HF/6-31G*)/CHARMM minimizations are more accurate than those at the (HF/3-21G)/CHARMM level they lead to the same conclusions. In the following discussion, only the (HF/6-31G*)/CHARMM results are presented.

Table 1. Natural bond order (*NBO*) atomic charges of the reactive atoms of the three stationary points along the reaction pathway

Atom name	3-21G				6-31G*			
	EA-1	EA-2	TI2	EP	EA-1	EA-2	TI2	EP
O_{acyl}	−0.80	−0.79	−0.87	−0.76	−0.87	−0.86	−0.97	−0.81
$N^{\varepsilon 2}$	−0.62	−0.62	−0.65	−0.64	−0.65	−0.65	−0.59	−0.66
O^{γ}	−0.61	−0.61	−0.67	−0.81	−0.64	−0.64	−0.73	−0.85
O_{wat}	−1.02	−1.04	−0.95	−0.79	−1.08	−1.10	−1.06	−0.81
H^1_{wat}	0.50	0.51	0.51	0.49	0.53	0.54	0.52	0.52
H^2_{wat}	0.49	0.46	0.48	0.55	0.53	0.51	0.50	0.56

Table 2. NBOs between selected pairs of atoms involved in the reaction

NBO		3-21G				6-31G*			
		EA-1	EA-2	TI2	EP	EA-1	EA-2	TI2	EP
O_{acyl}	H^N_{195}	0.03	0.02	0.06	0.00	0.02	0.01	0.04	0.00
O_{acyl}	H^N_{193}	0.07	0.05	0.12	0.07	0.04	0.03	0.08	0.03
O_{wat}	H^1_{wat}	0.55	0.54	0.16	0.00	0.58	0.57	0.11	0.00
O_{wat}	C_{acyl}	0.00	0.00	0.68	0.86	0.00	0.00	0.66	0.91
$N^{\varepsilon 2}$	H^1_{wat}	0.09	0.08	0.57	0.07	0.06	0.06	0.62	0.05
H^1_{wat}	O^{γ}	0.00	0.00	0.00	0.55	0.00	0.00	0.00	0.58
C_{acyl}	O_{acyl}	1.13	1.12	0.99	1.17	1.24	1.24	1.08	1.28
C_{acyl}	O^{γ}	0.88	0.89	0.74	0.01	0.95	0.95	0.79	0.00

3.1 Acyl-enzyme

To understand the nature of the binding of the hydrolytic water in the EA active site, two minimized model structures of the EA were analyzed (EA-1 and EA-2). They differ only in the location of the hydrolytic water (Fig. 2). In EA-1, the water is hydrogen bonded to the catalytic nitrogen atom of His-57 ($N^{\varepsilon 2}$) and to bulk water, while in EA-2 it forms a hydrogen-bonded bridge between $N^{\varepsilon 2}$ and the carbonyl oxygen, as in the crystal structure of the EA indoleacryloyl-α-chymotrypsin [6].

A comparison of the two models of the EA intermediate does not show any significant difference in the atomic charges or in the bond orders of the reactive atoms. The N—O distance between $N^{\varepsilon 2}$ of His-57 and the hydrolytic water oxygen (O_{wat}) is 2.9 Å in both structures, which is similar to the average distance of 3.1 Å observed in a previous MD simulation [23]. In both EA-1 and EA-2, H^1_{wat} is hydrogen bonded to $N^{\varepsilon 2}$ with an N—H distance of 2.0 Å. However, H^2_{wat} is not hydrogen bonded with an equal distance: in EA-1 it is hydrogen bonded to a bulk water molecule with an O—H distance of 1.7 Å, while in EA-2 it is hydrogen bonded to O_{acyl} with an O—H distance of 1.95 Å. The O—C distances, between the water oxygen (O_{wat}) and the carbonyl carbon (C_{acyl}), are 3.2 and 3.3 Å in EA-1 and EA-2, respectively. These distances, which are shorter than those found in earlier simulations (3.9 Å) [23], are reasonable considering that O_{wat} is poised to attack C_{acyl} for deacylation.

In both EA structures, the carbonyl oxygen (O_{acyl}) is located in the oxyanion hole, 9° above the plane defined by C_{acyl} and the two amide hydrogens of Gly-193 and Ser-195 (H^N_{193} and H^N_{195}), with an C—O bond order of 1.24. This result is consistent with structural studies of subtilisin and elastase [18, 21] but not with the crystal

Table 3. Selected distances and angles in the reaction region

Distance (Å)		3-21G				6-31G*			
		EA-1	EA-2	TI2	EP	EA-1	EA-2	TI2	EP
O_{acyl}	H^N_{195}	2.18	2.33	2.00	3.36	2.25	2.37	2.11	3.39
O_{acyl}	H^N_{193}	1.84	1.99	1.68	1.83	1.92	1.99	1.78	1.89
O_{wat}	H^1_{wat}	0.98	0.98	1.55	2.74	0.96	0.96	1.67	2.80
O_{wat}	$N^{\varepsilon 2}$	2.82	2.92	2.60	3.11	2.89	2.94	2.69	3.15
O_{wat}	C_{acyl}	3.09	3.32	1.57	1.33	3.18	3.32	1.54	1.31
$N^{\varepsilon 2}$	C_{acyl}	3.69	3.46	3.44	3.75	3.70	3.48	3.49	3.76
$N^{\varepsilon 2}$	H^1_{wat}	1.90	1.93	1.05	1.91	2.00	1.98	1.03	1.96
O_{acyl}	H^2_{wat}	4.23	1.93	2.98	3.02	4.26	1.95	2.88	2.97
$N^{\varepsilon 2}$	O^{γ}	3.18	3.18	2.97	2.82	3.23	3.22	3.02	2.84
H^1_{wat}	O^{γ}	3.03	3.47	2.37	0.98	3.14	3.49	2.40	0.96
C_{acyl}	O_{acyl}	1.22	1.29	1.32	1.22	1.22	1.22	1.29	1.20
C_{acyl}	O^{γ}	1.32	1.32	1.42	2.97	1.29	1.30	1.40	3.02
Angle (degree)									
O_{wat} O_{acyl}	C_{acyl}	87	58	110	119	85	58	109	118
C_{acyl} H^N_{195}	H^N_{193} O_{acyl}	9	9	4	−6	8	9	4	−7

structure of indoleacryloyl-α-chymotrypsin [6]. In the latter, O_{acyl} is not bound in the oxyanion hole and the water is not optimally positioned to attack the carbonyl unless O_{acyl} swings into the hydrogen-bonding site between Ser-195 and Gly-193. In EA-1, the hydrogen bond that O_{acyl} creates with the backbone NH group of Gly-193 (1.9 Å) is shorter than that formed with the backbone NH group of Ser-195 (2.3 Å). In EA-2, O_{acyl} is hydrogen bonded to H^{N}_{193} (2.0 Å) and to the hydrolytic water (2.0 Å) and, therefore, it cannot form a hydrogen bond with the backbone NH group of Ser-195. The angle O_{wat}-C_{acyl}-O_{acyl} is 85° in EA-1 versus 58° in EA-2. The optimal value of this angle for nucleophilic attack on an acyl group is about 107° [43]. On the basis of these results, the hydrolytic water molecule of EA-1, which is hydrogen bonded to $N^{\varepsilon 2}$ and to bulk water, is more likely to be in a suitable position for attack on the carbonyl carbon.

EA-1 is 2 kcalmol^{-1} lower in energy than EA-2 at the (HF/6-31G*)/CHARMM level. The small energy difference between the two minima could explain the fact that the hydrolytic water is found in different positions in different crystal structures [6, 21].

3.2 Tetrahedral intermediate

The deacylation is initiated by the attack of a water molecule on the EA carbonyl group. The nucleophilic attack of the hydrolytic water molecule on the EA carbonyl carbon has been suggested to lead to a TI2. The TI2 does not accumulate during the course of the reaction [44, 45] and the evidence for its existence in both acylation and deacylation steps is circumstantial [27]. However, tetrahedral structures have been observed in complexes of serine proteases with transition-state analogues; for example, ones which contain aldehyde groups in place of the carbonyl position of the scissile bond [25, 26].

We modeled the TI2 of the deacylation step. The intermediate state is destabilized by 28 kcalmol^{-1} relative to the EA at the (HF/6-31G*)/CHARMM level. The structure is found to be a weakly bonded system owing to the change from a planar ester bond to a tetrahedral system with three C—O bonds around the carbonyl carbon (C_{acyl}). The C—O bond order between C_{acyl} and O_{acyl} in the TI2 is smaller than in the EA (1.08 versus 1.24) and the bond is elongated by 0.07 Å (1.29 versus 1.22 Å). The C—O bond order between C_{acyl} and O^{γ} is also smaller in the TI2 relative to the EA (0.79 in TI2 versus 0.95 in EA-1), which correlates well with a longer bond (1.4 Å in TI2 versus 1.3 Å in EA-1). The bond order between the peptide carbonyl carbon (C_{acyl}) and the oxygen which originates from the hydrolytic water molecule (O_{wat}), is 0.66. O_{wat} is strongly hydrogen bonded (bond order 0.11, distance 1.7 Å) to the hydrogen on $N^{\varepsilon 2}$ of His-57 (H^{1}_{wat}).

The carbonyl oxygen (O_{acyl}) in the minimized structure of the TI2 occupies its proposed position between the backbone NH groups of Gly-193 and Ser-195 in the oxyanion hole. The negative charge on O_{acyl} is greater in the TI2 than in the EA (−0.97*e* versus −0.87*e*), owing to charge transfer from the deprotonated water. As a result, the hydrogen bonds between O_{acyl} and the backbone NH groups of Ser-195 and Gly-193 are shorter in the TI2 than in the EA (2.1 and 1.8 Å in TI2 versus 2.3 and 1.9 Å in EA-1). The bond orders of the corresponding hydrogen bonds are 0.04 and 0.08 versus 0.02 and 0.04 in TI2 and EA-1, respectively. The dihedral angle O_{acyl} creates with the plane of the carbonyl carbon and the two amide hydrogens is smaller than in the EA (4° versus 8°).

To complete the reaction, the acyl bond between O^{γ} of Ser-195 and the carbonyl carbon must be broken to release the cleaved peptide. This step can happen by a proton transfer from $N^{\varepsilon 2}$ of the imidazolium ring to O^{γ}, which necessitates that the ring gets closer to Ser-195. The mobility of the general acid-catalyst histidine is shown by our results, although it is relatively low, the distance between $N^{\varepsilon 2}$ and O^{γ} is shorter in the TI2 than in the EA (3.0 versus 3.2 Å), and the imidazolium proton (H^{1}_{wat}) is close to O^{γ} in the TI2, with a distance of 2.4 Å.

3.3 EP complex

During the final step of the reaction, the cleaved peptide leaves the active site. In contrast to a previous theoretical study [22], the carbonyl oxygen (O_{acyl}) of the EP complex is not hydrogen bonded to the backbone hydrogen of Ser-195 (H^{N}_{195}) (3.4 Å), but only to H^{N}_{195} (1.9 Å), and it moves 7° below the plane created by the carbonyl carbon (C_{acyl}) and the two amide hydrogens. C_{acyl} is further away from $N^{\varepsilon 2}$ of the imidazole ring than in the TI2 (3.8 versus 3.5 Å). These results suggest that the peptide can be expelled more easily if the carbonyl oxygen is not strongly hydrogen bonded in the oxyanion hole. The EP is destabilized by 5 kcalmol^{-1} relative to the EA at the (HF/6-31G*)/CHARMM level; however, the final products (free enzyme and solvated peptide) are probably lower in energy.

In comparison with the TI2, the distance between $N^{\varepsilon 2}$ and O^{γ} of Ser-195 was found to be shorter in the EP complex than in the TI2 (2.8 versus 3.0 Å). The hydrogen on O^{γ}, which originates from the imidazolium ring (H^{1}_{wat}), is hydrogen bonded to $N^{\varepsilon 2}$ with a distance of 2.0 Å and a bond order of 0.05.

4 Conclusions

Most of the work concerning the catalytic mechanism of serine proteases has focused on the first part of the catalytic step, leading to the EA. In this work we employed QM/MM minimizations on three stationary points along the second part of the catalytic step, the deacylation step, assuming a stepwise mechanism.

Our model is based on a recent high-resolution crystal structure of the EA intermediate [21]. What emerges from the present study is that the nucleophilic water in the EA has at least two minima in which it is held strongly by hydrogen bonds. The water can populate

both minima owing to the small energy difference between them. In both EA structures, the carbonyl group is located in the oxyanion hole, which positions it for an attack by the hydrolytic water.

The bonds of the tetrahedral system are weak, which destabilizes it relative to the EA. However, the carbonyl oxygen in the TI2 forms shorter hydrogen bonds with the backbone NH groups of Ser-195 and Gly-193 than in the EA. This result supports the hypothesis that the electrostatic stabilization of the negatively charged TI2 by main-chain dipoles in the oxyanion hole is an important factor in the mechanism [13].

The short distance between $N^{\varepsilon 2}$ of His-57 and O^{γ} of Ser-195 in the TI2 indicates a small movement of the imidazole ring towards the product during the deacylation step, which is important for its action as a good general base-acid catalyst.

The carbonyl group of the EP complex is not held strongly in the oxyanion hole, which suggests that the peptide is first released from the oxyanion hole before it leaves the active site and the native state of the enzyme is regenerated.

Although the present minimizations give important information on the deacylation step with the use of an ab initio QM/MM potential, they deal only with stationary points along the reaction pathway. A QM/MM dynamics simulation will enable us to examine the fluctuations in the active site and to evaluate the free-energy changes in the reaction. The present study shows that the results from the minimizations at the (HF/3-21G)/CHARMM level are similar to those at the (HF/6-31G*)/CHARMM level and, therefore, the use of the (HF/3–21G)/CHARMM potential is sufficient for subsequent MD simulations.

Acknowledgements. We are grateful to Aaron R. Dinner and Christopher J. Schofield for helpful discussions. M.T. is funded by the Wingate Scholarships and the Overseas Research Students Awards Scheme. The work was, in part, supported by a grant from the National Foundation for Cancer Research. We thank the Oxford Supercomputing Centre for the generous allocation of computer time.

References

1. Fersht A (1998) Structure and mechanism in protein science. Freeman, New York
2. Goldblum A (1997) In: Náray-Szabó G, Náray-Szabó AW (eds) Computational approaches to biochemcal reactivity. Kluwer, Amsterdam, p 295–340
3. Blow DM, Birktoft JJ, Hartley BS (1969) Nature 221: 337–340
4. Blow DM (1976) Acc Chem Res 9: 145–152
5. Bender ML, Killheffer JV (1973) Crit Rev Biochem Mol Biol 1: 149–199
6. Henderson R (1970) J Mol Biol 54: 341–354
7. Robertus JD, Kraut J, Alden RA, Birktoft J (1972) Biochemistry 11: 4293
8. Kraut J (1977) Annu Rev Biochem 46: 331–358
9. Nakagawa S, Umeyama H (1984) J Mol Biol 179: 103–123
10. Bizzozero SA, Dutler H (1981) Bioorg Chem 10: 46–62
11. Bachovchin WW (1986) Biochemistry 25: 7751–7759
12. Sumi H, Ulstrup J (1988) Biochim Biophys Acta 955: 26–42
13. Warshel A, Russell S (1986) J Am Chem Soc 108: 6569–6579
14. Frey PA, Whitt SA, Tobin JB (1994) Science 264: 1927–1930
15. Warshel A, Papazyan A (1996) Proc Natl Acad Sci USA 93: 13665–13670
16. Cassidy CS, Lin J, Frey PA (1997) Biochemistry 36: 4576–4584
17. Ash EL, Sudmeier JL, De Fabo EC, Bachovchin WW (1997) Science 278: 1128–1132
18. Tonge PJ, Carey PR (1990) Biochemistry 29: 10723–10727
19. Tonge PJ, Carey PR (1992) Biochemistry 31: 9122–9125
20. Whiting AK, Peticolas WL (1994) Biochemistry 33: 552–561
21. Wilmouth RC, Clifton IJ, Robinson CV, Roach PL, Aplin RT, Westwood NJ, Hajdu J, Schofield CJ (1997) Nature Struct Biol 4: 456–462
22. Daggett V, Schroeder S, Kollman P (1991) J Am Chem Soc 113: 8926–8935
23. Nakagawa S, Yu H-A, Karplus M, Umeyama H (1993) Proteins 16: 172–194
24. Komiyama M, Bender ML (1979) Proc Natl Acad Sci USA 76: 557–560
25. Brayer GD, Delbaere LT, James MN, Bauer CA, Thompson RC (1979) Proc Natl Acad Sci USA 76: 96–100
26. Delbaere LT, Brayer GD (1980) J Mol Biol 139: 45–51
27. Markley JL, Travers F, Balny C (1981) Eur J Biochem 120: 477–485
28. Stanton RV, Perakyla M, Bakowies D, Kollman PA (1998) J Am Chem Soc 120: 3448–3457
29. Warshel A, Levitt M (1976) J Mol Biol 103: 227–249
30. Field MJ, Bash PA, Karplus MA (1990) J Comput Chem 11: 700–733
31. Bernstein FC, Koetzle TF, William GJB, Meyer EJ Jr, Brice MD, Rogers JR, Kennerd O, Shimanouchi T (1977) J Mol Biol 112: 532–542
32. Brooks BR, Bruccoleri RE, Olafson BD, States DJ, Swaminathan S, Karplus M (1983) J Comput Chem 4: 187–217
33. MacKerell AD, Bashford D, Bellott M, Dunbrack RL, Evanseck JD, Field MJ, Fischer S, Gao J, Guo H, Ha S, Joseph-McCarthy D, Kuchnir L, Kuczera K, Lau FTK, Mattos C, Michnick S, Ngo T, Nguyen DT, Prodhom B, Reiher WE, Roux B, Schlenkrich M, Smith JC, Stote R, Straub J, Watanabe M, Wiorkiewicz-Kuczera J, Yin D, Karplus M (1998) J Phys Chem B 102: 3586–3616
34. Besler BH, Merz KM, Kollman PA (1990) J Comput Chem 11: 431–439
35. Frisch MJ, Trucks GW, Schlegel HB, Scuseria GE, Robb MA, Cheeseman JR, Zakrzewski VG, Montgomery JA, Stratmann RE, Burant JC, Dapprich S, Millam JM, Daniels AD, Kudin KN, Strain MC, Farkas O, Tomasi J, Barone V, Cossi M, Cammi R, Mennucci B, Pomelli C, Adamo C, Clifford S, Ochterski J, Petersson GA, Ayala PY, Cui Q, Morokuma K, Malick DK, Rabuck AD, Raghavachari K, Foresman JB, Cioslowski J, Ortiz JV, Stefanov BB, Liu G, Liashenko A, Piskorz P, Komaromi I, Gomperts R, Martin RL, Fox DJ, Keith T, Al-Laham MA, Peng CY, Nanayakkara A, Gonzalez C, Challacombe M, Gill PMW, Johnson BG, Chen W, Wong MW, Andres JL, Head-Gordon M, Replogle ES, Pople JA (1998) Gaussian 98, revision A.3. Gaussian, Pittsburgh, Pa
36. Jorgensen WL, Chandrasekhar J, Madura JD, Impey RW, Klein ML (1983) J Chem Phys 79: 926–935
37. Brook CL III, Karplus M (1989) J Mol Biol 208: 159–181
38. Brunger AT, Huber R, Karplus M (1987) Biochemistry 26: 5153–5162
39. Gunsteren WF, Berendsen HJC (1977) Mol Phys 34: 1311
40. Schmidt MW, Baldridge KK, Boatz JA, Elbert ST, Gordon MS, Jensen JH, Koseki S, Matsunaga N, Nguyen KA, Su S, Windus TL, Dupuis M, Montgomery JA Jr (1993) J Comput Chem 14: 1347–1363
41. Eurenius KP, Chatfield DC, Brooks BR, Hodoscek M (1996) Int J Quantum Chem 60: 1189
42. Reed AE, Curtiss LA, Weinhold F (1988) Chem Rev 88: 899
43. Burgi HB, Lehn JM, Wipff G (1974) J Am Chem Soc 96: 1956–1957
44. Fersht AR, Renard M (1974) Biochemistry 13: 1416–1426
45. Fastrez J, Fersht AR (1973) Biochemistry 12: 1067–1074